Anomalous structure-property relationships in metallic glasses through pressure-mediated glass formation

Jun Ding,[1] Mark Asta,[1,2,*] and Robert O. Ritchie[1,2,†]

[1]*Materials Sciences Division, Lawrence Berkeley National Laboratory, Berkeley, California 94720, USA*
[2]*Department of Materials Science and Engineering, University of California, Berkeley, California 94720, USA*

Metallic glasses are commonly found to favor denser packing structures and icosahedral order in experiments, simulations, and theoretical models. Here we present a molecular dynamics simulation study of Cu-Zr metallic glasses, prepared through a pressure-mediated pathway. The resulting glasses exhibit anomalous structure-property relationships; these glasses are less energetically stable, concomitant with a denser atomic packing and a significant increase in icosahedral short-range order. The enhanced icosahedral order is shown to be accompanied by a pressure-mediated change in chemical short-range order. The results demonstrate that in amorphous alloys (nonmonatomic), theoretical frameworks of the two-order-parameter model must be generalized to account for chemical degrees of freedom.

Since their discovery several decades ago [1], metallic glasses (MGs), or amorphous alloys, have attracted significant interest in the academic and industrial communities due to their unique combination of properties [2–5]. In contrast to other amorphous materials, e.g., silica, soda-lime-silica, or chalcogenide glasses, MGs display a close-packed atomic structure with typically 12 nearest-neighbor atoms [6–8] while network glasses are normally loosely packed with a much lower coordination number of 3–6 [9–11], reflecting their preferred bonding geometries. For the dense atomic packing that is characteristic of MGs, there are two key structural indicators that commonly reflect the stability of the glassy state: the atomic volume (related to the concept of free volume or atomic density) [12–22] and icosahedral short-range order (ISRO) [6–8,23–29]. Specifically, in both experiments and computer simulations, it is widely found that slower cooling and/or longer aging generally leads to MGs with lower volume (higher density) [12–18] and increased icosahedral short-to-medium-range order [8]. In addition, volume expansion and increasing distortion (or fragmentation) of atomic clusters are typically observed in the rejuvenation of MGs undergoing shear deformation [8,19,20,26] or ion irradiation [21]. Consistent with these observations, most theoretical structural models of metallic glasses are derived from the concept of efficient packing with icosahedral clusters [6–8,25]. In comparison, the atomic density of oxide or network glasses is more complex. For instance, silica glasses (SiO_2) have been shown to undergo a volume dilation with annealing or with slower quenching rates [30], but become denser under irradiation with an associated increase in internal energy [31]; both observations are in marked contrast with the general behavior of MGs.

In this Rapid Communication, we present a computer-simulation study of Cu-Zr MGs that provides insights into the relationship between the atomic structure and the properties of MGs. Through a processing path involving pressure-mediated glass formation, we demonstrate amorphous alloys with structure-property relationships that are anomalous, in the

sense that glasses which simultaneously display lower atomic volume (higher atomic density), and increased ISRO, are associated with *lower* energetic stability (i.e., higher potential energy): Such an anomalous structure-property relationship can be understood as resulting from the pressure-mediated change in the preferred state of a combination of topological and chemical short-range order (CSRO). The implications of these findings are discussed in the framework of commonly employed two-order-parameter models [32,33], which we show must be generalized to include the role of CSRO in dictating locally preferred structures, to provide a more complete description of structure-property relations in amorphous alloys.

Two pathways of glass formation are employed in the present work to prepare MG samples by computer simulations: (i) Path I involves a quench from the liquid to glassy state at ambient pressure—this is the regular mode of glass formation considered in most computational and experimental investigations; (ii) path II involves the application of a hydrostatic pressure during quenching, followed by the release of the imposed pressure once the material is at room temperature (Fig. 1), which is distinct from previous studies of applied pressure on glasses and liquids [34–40] in the context of investigations of liquid-liquid transitions, polyamorphism, and pressure-induced amorphization/crystallization.

In the current study, Cu-Zr MGs with two different compositions ($Cu_{50}Zr_{50}$ and $Cu_{64}Zr_{36}$), each containing 16000 atoms, were analyzed using molecular dynamics (MD) simulations [41] based on an optimized embedded-atom-method interatomic potential [27]. For both $Cu_{50}Zr_{50}$ and $Cu_{64}Zr_{36}$ MGs, the same simulation procedure was employed with both glasses exhibiting similar results. Accordingly, only results from the $Cu_{50}Zr_{50}$ MGs are presented below; corresponding results for the $Cu_{64}Zr_{36}$ glass can be found in the Supplemental Material [42]. The simulation samples were prepared in three separate stages, as illustrated in Fig. 1: (i) Liquids at a specific applied hydrostatic pressure ($P = -5$ to 20 GPa) were equilibrated at high temperature, then (ii) quenched to room temperature (300 K) with a cooling rate of 10^{11} K/s, and finally (iii) the applied hydrostatic pressure was released and the MGs were allowed to relax for 100 ns at room temperature. For comparison, "regular" $Cu_{50}Zr_{50}$ MGs were also prepared by
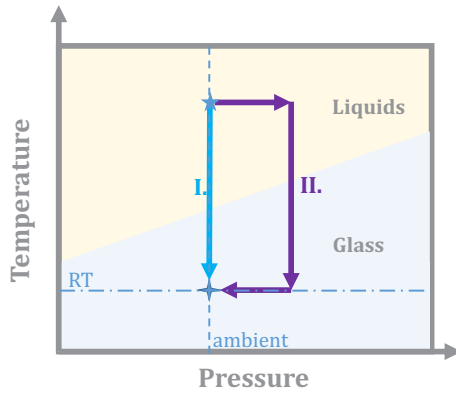
*mdasta@berkeley.edu
†roritchie@lbl.gov

FIG. 1. Schematic illustration of the two pathways to glass formation employed in the computer simulation studies: (I) through fast quenching at ambient pressure; (II) via quenching of the (hydrostatic) pressurized liquid to achieve a glassy state, followed by the release of the external pressure at room temperature (RT).

cooling at rates of 10^9–10^{12} K/s, using zero applied pressure (path I). The properties of each of the resulting MG samples were analyzed at ambient pressure. Hereafter we denote the different samples according to the value of the pressure imposed during glass formation.

The computed variation in potential energy (PE) with temperature for the three quenching processes with applied

pressures of $P = 0, -5$, and 10 GPa are shown in Fig. 2(a) for a constant cooling rate of 10^{11} K/s. We note that in the liquid state the potential energy is lowest for the sample at $P = 10$ GPa; the relative energetic stability of these samples switches, however, after glass formation and relaxation to zero pressure. Figure 2(b) shows the temperature- and pressure-dependent fraction of Cu-centered full icosahedra (i.e., with a Voronoi index $\langle 0,0,12,0 \rangle$) using Voronoi tessellation analysis to identify the topological packing of nearest neighbors [8]. The effects of applied hydrostatic pressure on ISRO are twofold in Fig. 2(b): First, increasing P enhances the ISRO at the same temperature; second, at higher P, there is an enhanced rate of increase of ISRO with decreasing T during the liquid-glass transition. Moreover, the ISRO is found to undergo a pronounced increase during quenching close to the corresponding glass-transition temperatures T_g, as marked in Fig. 2(a).

The higher the P, the greater is the T_g at the same cooling rate, as confirmed in Fig. 2(c), which is consistent with the analysis of pressure-dependent liquid dynamics, such as diffusion and α-relaxation time (see Figs. S1 and S2 [42]): P can slow down the dynamics of the melts [43], allowing glass formation to occur at higher temperatures at the same cooling rate. Interestingly, the Cu-Zr liquids become more fragile with higher P (Fig. S3 [42]), which is consistent with (i) previous theoretical studies [44,45], and (ii) the steeper
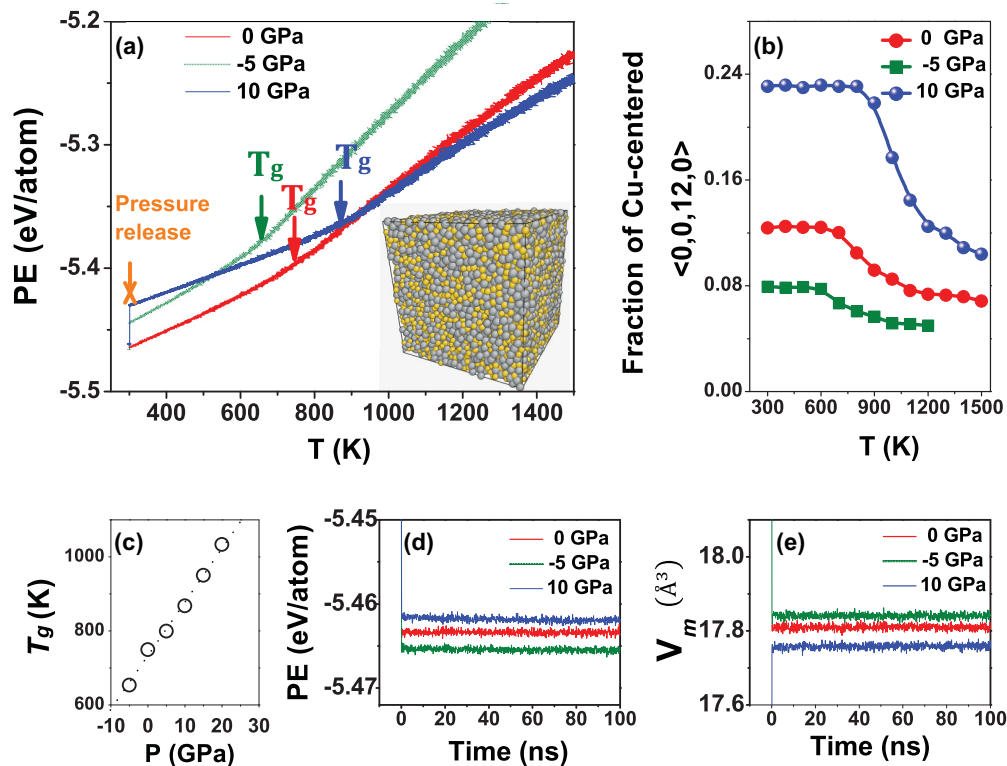

FIG. 2. (a) Variation in potential energy (PE) with temperature for three representative $Cu_{50}Zr_{50}$ MGs quenched from a high-temperature liquid state with applied hydrostatic pressure values of $P = 0$ (regular quenching), 10, and -5 GPa, respectively, at a cooling rate of 10^{11} K/s. The applied pressure is released at 300 K, as marked, and relaxation is maintained for 100 ns. The inset shows the atomic configuration of the $Cu_{50}Zr_{50}$ MG (at $P = 10$ GPa); yellow spheres are Cu atoms and gray spheres are Zr atoms. (b) The temperature- and pressure-dependent fraction of Cu-centered full icosahedra $\langle 0,0,12,0 \rangle$. (c) Variation in the glass transition temperature T_g with applied hydrostatic pressure. (d) and (e) Respective variations in potential energy and atomic volume with relaxation at 300 K.
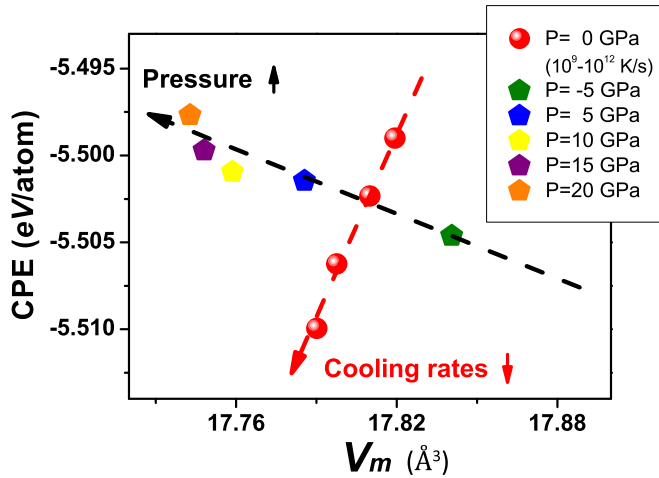
FIG. 3. Configurational potential energy (CPE) as a function of atomic volume for $Cu_{50}Zr_{50}$ MGs quenched at a cooling rate of $10^{11} K/s$ and applied hydrostatic pressure of $P = -5$ to 20 GPa. By comparison, regular quenched $Cu_{50}Zr_{50}$ MGs (with $P = 0$) are also shown with data points as red spheres for cooling rates from 10^9 to $10^{12} K/s$. The black and red arrows indicate, respectively, the directions of increasing pressure and slower cooling rates.

rate of increase of ISRO upon undercooling in Fig. 2(b) [46,47].

After removing the applied pressure and relaxing the samples at 300 K, the PE for the $Cu_{50}Zr_{50}$ MGs at $P = 10$ and -5 GPa undergoes a sudden drop [Fig. 2(d)]. At ambient pressure and temperature, the relationship between the final PE and atomic volume (V_m) is anomalous for these three samples [see Figs. 2(d) and 2(e)], in the sense that the sample with the highest density ($P = 10$ GPa) is least favored energetically. Figure 3 shows the computed configurational potential energy (CPE) [12] as a function of V_m for the $Cu_{50}Zr_{50}$ MGs (see Fig. S4 for a slower cooling rate of $10^{10} K/s$ [42]); the different P and cooling rates employed during the quenching process are delineated, respectively. Two opposite V_m- CPE relationships are observed. For the "normal" pathway to glass formation ($P = 0$), smaller values of V_m correlate with a lower state of internal energy, as expected. By contrast, for the pressure-mediated pathway to glass formation, the relationship between V_m and CPE for MGs prepared with the same cooling rate is inversely related. Interestingly, the higher density glasses obtained through the pressure-mediated pathway display an almost unchanged shear modulus (Fig. S5 [42]), which could reflect a balance between higher internal energy (according to the Johnson-Samwer cooperative shear model [2]) and higher density [48].

We note that the inverse volume-energy relationship for pressure-mediated metallic-glass formation (Fig. 3) has been already observed in other glassy materials, especially oxide or network glasses [49–51]. But, as discussed above, MGs have close-packed atomic structures, and their volume is generally observed to be *directly* and *strongly* associated with energetic stability in nearly all of the existing experiments, computer simulations, and theories. Thus, for a more general understanding of structure-property relations in MGs, it is of interest to explain the anomalous volume-energy relation displayed in Fig. 3.
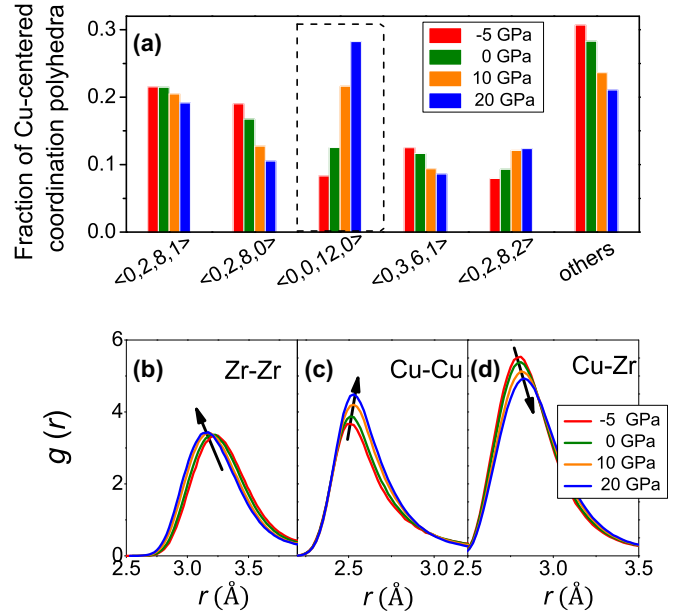

FIG. 4. $Cu_{50}Zr_{50}$ MGs quenched at different hydrostatic pressures, $P = -5, 0, 10$, and 20 GPa at a cooling rate of $10^{11} K/s$, showing (a) the fraction of Cu-centered coordination polyhedra with a Voronoi index for the most common atomic motifs; (b)–(d) partial pair correlation functions for Zr-Zr, Cu-Cu, and Cu-Zr pairs, respectively (arrows indicate the direction of the shift in peak position with increasing applied pressure).

We thus consider the nature of the ISRO within the different Cu-Zr MGs at ambient pressure and room temperature, prepared with, and without, applied pressure during quenching. The icosahedral order is generally accepted as the key structural feature in MGs [6–8,23–29], while the role of crystal-like order is still under debate [52,53]. Figure 4(a) shows the fraction of Cu-centered coordination polyhedra with the most commonly observed atomic motifs in $Cu_{50}Zr_{50}$ MGs: $\langle 0,2,8,1 \rangle$, $\langle 0,2,8,0 \rangle$, $\langle 0,0,12,0 \rangle$, $\langle 0,3,6,1 \rangle$, and $\langle 0,2,8,2 \rangle$ [8]. The fractions of the various atomic motifs are found to vary with P [Fig. 4(a)]. The most pronounced and interesting changes are for the $\langle 0,0,12,0 \rangle$ atomic motif, which increases from 8.3% to 28.3% as the applied pressure varies from -5 to 20 GPa; the results are consistent with the temperature-dependent results shown in Fig. 2(b) for different imposed pressures. As extensively studied elsewhere [8,28], the $\langle 0,0,12,0 \rangle$ motif, referred to as a full icosahedron, is regarded as being the most favored in certain Cu-Zr MGs, in particular, for Cu-rich compositions. The presence of this atomic motif is strongly correlated with specific properties of these metallic glasses and liquids, such as the slowing of liquid dynamics and the formation of a "backbone" that impedes shear deformation [8,26–28,54].

Note that the fraction of the $\langle 0,0,12,0 \rangle$ motif in $Cu_{50}Zr_{50}$ MGs increases only slightly with slower cooling rates for regularly quenched samples (at $P = 0$); maximum values of $\sim 14.5\%$ are achieved with the slowest cooling rate of 10^9 K/s (Fig. S7 in Ref. [42]). By comparison, the corresponding analysis of the $Cu_{64}Zr_{36}$ MGs, known as full-icosahedral dominated samples, are presented in Ref. [42]. The fraction of the Cu-centered $\langle 0,0,12,0 \rangle$ motif in these MGs increases from

TABLE I. Total and species-dependent coordination numbers (CN) around Cu and Zr atoms for $Cu_{50}Zr_{50}$ MGs quenched with different applied pressures and cooling rates.

	10^{11}K/s $P = 20$ GPa	10^{11}K/s $P = 10$ GPa	10^{11}K/s $P = 0$ GPa	10^{10}K/s $P = 0$ GPa	10^{9}K/s $P = 0$ GPa
CN of Cu	**11.26**	**11.14**	**10.89**	**10.91**	**10.92**
(Cu)	(4.26)	(4.09)	(3.81)	(3.81)	(3.80)
(Zr)	(7.00)	(7.05)	(7.08)	(7.10)	(7.12)
CN of Zr	**14.50**	**14.56**	**14.67**	**14.69**	**14.73**
(Cu)	(7.00)	(7.05)	(7.09)	(7.10)	(7.12)
(Zr)	(7.50)	(7.51)	(7.58)	(7.59)	(7.61)

25% to 35% between $P = 0$ and 20 GPa at the same cooling rate of 10^{11}K/s. This increase in icosahedral order in the $Cu_{50}Zr_{50}$ and $Cu_{64}Zr_{36}$ MGs exposed to applied pressure during quenching occurs despite the fact that each glass becomes energetically less stable. The trend is thus in marked contrast to the generally accepted understanding of the effect of ISRO on the structure-property relationships in MGs. Furthermore, another pertinent structure indicator in amorphous alloys, the atomic-level pressure [55,56], is examined in Fig. S6 [42], which also exhibits an anomalous trend for MGs formed through pressure-mediated glass formation.

To summarize the key findings of the computer simulations, we have observed an anomalous structure-property relationship in Cu-Zr MGs reflected by the relationship between internal energy and two primary structural indicators: atomic volume and ISRO. Those structural indicators are influenced by the atomic bonding and coordination numbers (CNs) for nearest-neighbor pairs as detailed in the analysis in Figs. 4(b)–4(d), Table I, and the Supplemental Material [42], which characterize the distinct local atomic environments obtained via path I and II glass formation. For example, CSRO in MGs has been well studied in Refs. [6–8,25,28,46,47,57]. As a measure of the nature of the CSRO in Cu-Zr MGs in the present work, the number of Cu atoms surrounding a central Cu atom increases significantly, from 3.81 to 4.26, when P increases from 0 to 20 GPa (Table I). Compared to the influence of varying cooling rate at zero pressure (path I), the higher P tunes the local atomic environment in MGs by changing the average chemical composition and bond lengths associated with the local atomic environment. What results is a chemical and topological SRO that is locally favored in the liquid at the finite pressures considered.

With this additional insight, we discuss the current findings in the context of the classical two-order-parameter model (TOP) proposed by Tanaka, which has led to a unified description of the liquid-liquid transition, glass transition, waterlike anomalies, and crystallization [32,33]. The TOP model is based on a picture whereby (i) there exists distinct locally favored structures (LFSs) as state S and (ii) such structures are formed in a "sea" of normal liquid structures (ρ). Different values of energy (E), specific (or atomic) volume (v), and entropy (σ) [32] are associated with each state. The fraction of the LFS increases upon cooling due to the lower associated energy state.

For water or waterlike liquids [32,33], where $E_S < E_\rho$, $v_S > v_\rho, \sigma_S < \sigma_\rho$ (higher specific volume associated with the LFS that is characterized by tetrahedral order), the TOP model can explain their anomalies, e.g., the maximum density at 4 °C for water. However, for metallic glasses/liquids, the LFS is interpreted to be of icosahedral order, and the normal structure-property relations are consistent with $E_S < E_\rho, v_S < v_\rho, \sigma_S < \sigma_\rho$. Such relations would naturally lead to a situation where decreasing temperature and decreasing cooling rates lead to increasing ISRO (minimizing energy and lower entropy) and lower atomic volume, as observed for the MGs prepared through path I in the current work. In the same picture it would be expected that increasing P during quenching would lead to more LFS order [Figs. 2(b) and 4(a)], thus forming a glass with higher atomic density, enhanced ISRO, and decreased energy after pressure release. This picture is thus in contrast to the present simulations, and can be reconciled by considering the effect of pressure on the preferred LFS. As shown above, the SRO in the liquid is altered at finite pressures, giving rise to preferred clusters that have increased Cu atoms surrounding Cu (and vice versa) at finite P. However, this CSRO corresponds to a higher-energy state when the pressure on the glass is released at room temperature (with resultant bond length variation by stiffness difference [58]). The very slow diffusion kinetics at room temperature traps the glasses produced through the pressure-mediated path in an energetically unfavorable state of CSRO. Thus, to describe the behavior observed in this study, the TOP would need to be modified for amorphous alloys (nonmonatomic) to account for the effect of CSRO on the LFS at finite pressures. Support for this picture is provided by separate studies on elemental glasses discussed in the Supplemental Material (for Ta and Fe); for these systems where the chemistry of the clusters is fixed, *no* anomalous structure-property relationship is observed (see Fig. S15) [42] when glasses are prepared with and without an applied pressure during quenching.

Hence, the findings presented in this Rapid Communication underscore the need to discern atomic-level structural metrics of MGs to accurately establish structure-property relationships, considering the complex nature of the atomic packing compared to hard-sphere models. Further, the ideal atomic-level structure parameters in MGs should directly originate from the potential energy landscape, especially the energy barriers for β relaxation processes (thermally activated and stress activated) [59–61], and the corresponding structural metrics are best depicted in multidimensional space aided by advanced algorithms, e.g., machine learning [62], rather than a more limited set of structural indicators.

In conclusion, we reveal here anomalous atomic-level structure-property relationships for MGs prepared through a pressure-mediated processing path. The distinct configurational states that are achieved by such a process act to tune the local atomic environments, including both topological and chemical short-range order, in a manner that is unanticipated from previous studies of MGs prepared by quenching at zero pressure. Through the pressure-mediated pathway, Cu-Zr MGs become less energetically stable, while displaying (i) a higher atomic density, and (ii) a significant increase of

icosahedral short-range order. Such observations are contrary to the currently accepted theory and understanding of the atomic structure in MGs. The findings are discussed in terms of generalizations to the two-order-parameter model [32] and underscore the need for incorporating chemical and topological ordering on an equal footing to describe the properties observed in this study. Furthermore, the insights derived in this work suggest the potential for stress-tuned MG processing to achieve unique combinations of properties [63,64] with the goal of designing superior high-performance structural engineering materials.

[1] W. Klement, R. H. Willens, and P. Duwez, Nature (London) **187**, 869 (1960).

[2] W. L. Johnson and K. Samwer, Phys. Rev. Lett. **95**, 195501 (2005).

[3] A. Inoue, Acta Mater. **48**, 279 (2000).

[4] W. H. Wang, C. Dong, and C. H. Shek, Mater. Sci. Eng., R **44**, 45 (2004).

[5] M. D. Demetriou, M. E. Launey, G. Garrett, J. P. Schramm, D. C. Hofmann, W. L. Johnson, and R. O. Ritchie, Nat. Mater. **10**, 123 (2011).

[6] D. B. Miracle, Nat. Mater. **3**, 697 (2004).

[7] H. W. Sheng, W. K. Luo, F. M. Alamgir, J. M. Bai, and E. Ma, Nature (London) **439**, 419 (2006).

[8] Y. Q. Cheng and E. Ma, Prog. Mater. Sci. **56**, 379 (2011).

[9] R. Brückner, J. Non-Cryst. Solids **5**, 123 (1970).

[10] A. Tilocca and N. H. de Leeuw, J. Mater. Chem. **16**, 1950 (2006).

[11] D. Lencer, M. Salinga, and M. Wuttig, Adv. Mater. **23**, 2030 (2011).

[12] P. G. Debenedetti and F. H. Stillinger, Nature (London) **410**, 259 (2001).

[13] H. S. Chen, J. Appl. Phys. **49**, 3289 (1978).

[14] A. Slipenyuk and J. Eckert, Scr. Mater. **50**, 39 (2004).

[15] A. R. Yavari et al., Acta Mater. **53**, 1611 (2005).

[16] C. Nagel, K. Rätzke, E. Schmidtke, J. Wolff, U. Geyer, and F. Faupel, Phys. Rev. B **57**, 10224 (1998).

[17] Y. Q. Cheng and E. Ma, Appl. Phys. Lett. **93**, 051910 (2008).

[18] Y. Qi, T. Çağın, Y. Kimura, and W. A. Goddard III, Phys. Rev. B **59**, 3527 (1999).

[19] M. W. Chen, Annu. Rev. Mater. Res. **38**, 445 (2008).

[20] A. L. Greer, Y. Q. Cheng, and E. Ma, Mater. Sci. Eng., R **74**, 71 (2013).

[21] S. G. Mayr, Phys. Rev. B **71**, 144109 (2005).

[22] F. Spaepen, Acta Metall. **25**, 407 (1977).

[23] A. Hirata et al., Nat. Mater. **10**, 28 (2011).

[24] A. Hirata et al., Science **341**, 376 (2013).

[25] D. B. Miracle, Acta Mater. **54**, 4317 (2006).

[26] Y. Q. Cheng, A. J. Cao, H. W. Sheng, and E. Ma, Acta Mater. **56**, 5263 (2008).

[27] Y. Q. Cheng, E. Ma, and H. W. Sheng, Phys. Rev. Lett. **102**, 245501 (2009).

[28] J. Ding, Y. Q. Cheng, and E. Ma, Acta Mater. **69**, 343 (2014).

[29] Y. T. Shen, T. H. Kim, A. K. Gangopadhyay, and K. F. Kelton, Phys. Rev. Lett. **102**, 057801 (2009).

[30] L. Huang and J. Kieffer. Appl. Phys. Lett. **89**, 141915 (2006).

[31] A. Navrotsky, Rev. Mineral. **29**, 309 (1994).

[32] H. Tanaka, Eur. Phys. J. E **35**, 113 (2012).

[33] J. Russo and H. Tanaka, Nat. Commun. **5**, 3556 (2014).

[34] Y. Katayama, T. Mizutani, W. Utsumi, O. Shimomura, M. Yamakata, and K. Funakoshi, Nature (London) **403**, 170 (2000).

[35] M. Guthrie, C. A. Tulk, C. J. Benmore, J. Xu, J. L. Yarger, D. D. Klug, J. S. Tse, H.-k. Mao, and R. J. Hemley, Phys. Rev. Lett. **93**, 115502 (2004).

[36] H. W. Sheng et al., Nat. Mater. **6**, 192 (2007).

[37] Q. S. Zeng et al., Science **332**, 1404 (2011).

[38] R. J. Hemley, A. P. Jephcoat, H. K. Mao, L. C. Ming, and M. H. Manghnani, Nature (London) **334**, 52 (1988).

[39] S. K. Deb, M. Wilding, M. Somayazulu, and P. F. McMillan, Nature (London) **414**, 528 (2001).

[40] W. H. Wang, T. Okada, P. Wen, X. L. Wang, M. X. Pan, D. Q. Zhao, and W. Utsumi, Phys. Rev. B **68**, 184105 (2003).

[41] M. P. Allen and D. J. Tildesley, Computer Simulation of Liquids (Clarendon Press, Oxford, UK, 1987).

[42] See Supplemental Material at http://link.aps.org/supplemental/10.1103/PhysRevB.93.140204 for pressure dependence of liquid dynamics and other properties for metallic glasses made with applied pressure, which includes Refs. [65–69].

[43] D. Coslovich and C. M. Roland, J. Phys. Chem. B **112**, 1329 (2008).

[44] H. Shintani and H. Tanaka, Nat. Mater. **7**, 870 (2008).

[45] H. Tanaka, J. Chem. Phys. **111**, 3163 (1999).

[46] J. Ding, Y. Q. Cheng, H. W. Sheng, and E. Ma, Phys. Rev. B **85**, 060201 (2012).

[47] J. Ding, Y. Q. Cheng, and E. Ma, Acta Mater. **61**, 3130 (2013).

[48] W. H. Wang, Prog. Mater. Sci. **57**, 487 (2012).

[49] L. Wondraczek, S. Sen, H. Behrens, and R. E. Youngman, Phys. Rev. B **76**, 014202 (2007).

[50] L. Wondraczek, S. Krolikowski, and H. Behrens, J. Non-Cryst. Solids **356**, 1859 (2010).

[51] S. Pawlus, M. Paluch, J. Ziolo, and C. M. Roland, J. Phys.: Condens. Matter **21**, 332101 (2009).

[52] M. Leocmach and H. Tanaka, Nat. Commun. **3**, 974 (2012).

[53] J. Hwang, Z. H. Melgarejo, Y. E. Kalay, I. Kalay, M. J. Kramer, D. S. Stone, and P. M. Voyles, Phys. Rev. Lett. **108**, 195505 (2012).

[54] J. Ding, S. Patinent, M. L. Falk, Y. Q. Cheng, and E. Ma, Proc. Natl. Acad. Sci. USA **111**, 14052 (2014).

[55] T. Egami, Prog. Mater. Sci. **56**, 637 (2011).

[56] Y. Q. Cheng, J. Ding, and E. Ma, Mater. Res. Lett. **1**, 1 (2013).

[57] J. Ding and Y. Q. Cheng, Appl. Phys. Lett. **104**, 051903 (2014).

[58] H. W. Sheng, E. Ma, H. Z. Liu, and J. Wen, Appl. Phys. Lett. **88**, 171906 (2006).

[59] Y. Fan, T. Iwashita, and T. Egmai, Nat. Commun. **5**, 5083 (2014).

[60] H. B. Yu, W. H. Wang, and K. Samwer, Mater. Today **16**, 183 (2013).

[61] H. B. Yu, K. Samwer, Y. Wu, and W. H. Wang, Phys. Rev. Lett. **109**, 095508 (2012).

[62] E. D. Cubuk, S. S. Schoenholz, J. M. Rieser, B. D. Malone, J. Rottler, D. J. Durian, E. Kaxiras, and A. J. Liu, Phys. Rev. Lett. **114**, 108001 (2015).

[63] A. Concustell, S. Godard-Desmarest, M. A. Carpenter, N. Nishiyama, and A. L. Greer, Scr. Mater. **64**, 1091 (2011).

[64] D. C. Hofmann *et al.*, Nature (London) **451**, 1085 (2008).

[65] W. Kob and H. C. Andersen, Phys. Rev. E **52**, 4134 (1995).

[66] C. A. Angell, Science **267**, 1924 (1995).

[67] Y. Q. Cheng and E. Ma, Phys. Rev. B **80**, 064104 (2009).

[68] L. Zhong, J. Wang, H. W. Sheng, Z. Zhang, and S. X. Mao, Nature (London) **512**, 177 (2014).

[69] T. Iwashita, D. M. Nicholson, and T. Egami, Phys. Rev. Lett. **110**, 205504 (2013).